IET Communications

Research Article

IET Journals
The Institution of Engineering and Technology

Very high efficiency differential chaos shift keying system

ISSN 1751-8628
Received on 31st March 2016
Revised on 24th June 2016
Accepted on 16th July 2016
doi: 10.1049/iet-com.2016.0411
www.ietdl.org

Fadia Taleb[1] ✉, *Fethi Tarik Bendimerad*[1], *Daniel Roviras*[2]

[1]*Telecommunication Laboratory (LTT), Abou Bekr Belkaid University, CO 13000, Tlemcen, Algeria*
[2]*CEDRIC Laboratory, Conservatoire National des Arts et Métiers, Paris, France*
✉ *E-mail: taleb.fadia@gmail.com*

Abstract: In this study, a new non-coherent communication system, i.e. very high efficiency differential chaos shift keying system, is proposed. This system is a generalised form of the high efficiency differential chaos shift keying (HE-DCSK) system, with an arbitrary number (N) of transmitted bits per frame. The major advantage of this new proposition is its ability to significantly improve the spectral efficiency compared with DCSK and HE-DCSK. The theoretical bit error rate of this system is found using the Gaussian approximation method under different communication channels: additive white Gaussian noise and two-ray Rayleigh fading channels. Simulations in both environments show a perfect match with the analytical expressions for large spreading factors. Simulation results for the two-ray Rayleigh fading channel show clearly the diversity gain compared with the single-ray Rayleigh channel.

1 Introduction

Over the last decades, researchers have shown great interest in communication systems based on chaos. Many modulation and demodulation schemes have been proposed [1–13]. In [14], we find a comprehensive survey of all the wireless radio frequency chaos-based communication systems. Two main types of chaotic communication systems, widely studied, are worth mentioning: chaos shift keying (CSK) [1, 2] and differential CSK (DCSK) [3]. Several demodulation schemes exist for the CSK system, one of them is non-coherent and is based on the bit-energy estimation. The threshold-shift problem remains one of the drawbacks of this type of demodulation. The DCSK system has been suggested to facilitate the non-coherent detection and particularly to combat the problem of threshold shift in the non-coherent CSK system. In the DCSK system, each transmitted bit is represented by two chaotic sequences. The first one is a reference sequence, while the second acts as a carrier for the information. DCSK system has some drawbacks. The transmission rate is reduced by half, since it takes half the transmission time to transmit the reference sequence. Also, transmitting the same sequence twice may adversely affect security. To provide solutions to all these problems, at the expense of greater complexity, other systems were implemented thereafter. For example, in [4], the security of the DCSK system is enhanced by introducing permutations, which allow destroying the similarity that may exist between the reference sequence and the data-bearing sequence. In [5], a quadrature chaos shift keying system is proposed, where two perfectly orthogonal chaotic sequences, obtained by Hilbert transform, are used to transmit two bits of information in two consecutive time slots (TSs). This allows doubling the rate obtained by DCSK modulation at the expense of a higher complexity. The same bit rate is obtained in the improved DCSK system [6], by using a time-reversal operation to obtain two orthogonal signals, which will be used to transmit one bit of information in one TS. Moreover, M-ary DCSK [7] and differentially DCSK [8] are also proposed to enhance the data rate of the DCSK system. In [9], a secure multicarrier DCSK (MC-DCSK) is proposed to improve the security of the DCSK system. More recently, a new MC-DCSK was proposed in [10], where no RF delay line is needed. This system increases the spectral efficiency and uses less energy in comparison with DCSK. In [11], Xu and Wang propose the code shifted DCSK (CS-DCSK). In their proposal, the reference sequence and data-bearing sequence are separated by Walsh codes and are transmitted during the same TS. In [12], an extension of the CS-DCSK named high data rate DCSK is proposed to obtain a high data rate, where N bits of information are transmitted in the same TS. Only one reference sequence is used and transmitted, the other N chaotic sequences used to separate the N bits are supposed to be known from the receiver, making it a coherent system. In [13], Yang and Jiang suggest the high efficiency DCSK (HE-DCSK) system. In this system, a data frame consists of two equal length TSs. The first TS is allocated to a chaotic reference sequence. The second one allows transmitting two information bits by means of two data-bearing sequences. The performances are slightly better than DCSK ones in terms of data rate and bit error rate (BER), at reasonable noise levels.

In this work, we propose a generalisation of the HE-DCSK system, named very high efficiency differential chaos shift keying (VHE-DCSK). In this new system, a data frame is composed of two TSs. The first TS allows conveying the reference chaotic sequence, used to demodulate a portion of the transmitted information. The second one can convey N information bits. This ensures a bit rate N times higher, while occupying the same spectral bandwidth. It also ensures a security comparable to that of the system proposed in [4], without any additional blocks. Analytical expressions have been derived, showing very good agreement with simulation results. The new system is evaluated over an AWGN channel and over a two-ray Rayleigh fading channel. For the two-taps Rayleigh channel, the proposed system is able to exploit the diversity of order two.

The rest of this paper is organised as follows: In Section 2, a description of the VHE-DCSK transmitter scheme is given. In Section 3, we present the receiver scheme and we derive theoretical BER expressions for additive white Gaussian noise (AWGN) channel. In Section 4, we analyse BER performances using a two-ray Rayleigh fading channel. Simulation results are compared with theoretical ones in Section 5. A final conclusion is given in Section 6.

2 VHE-DCSK transmitter scheme

A generalised HE-DCSK communication system is proposed, as shown in Fig. 1. The structure of the transmitter consists of a

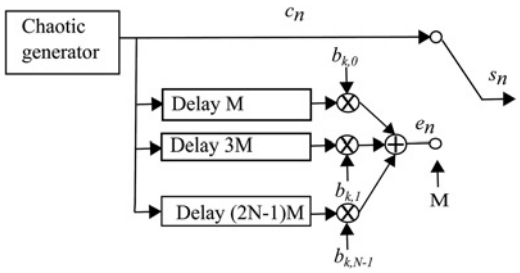

Fig. 1 *Transmitter structure*

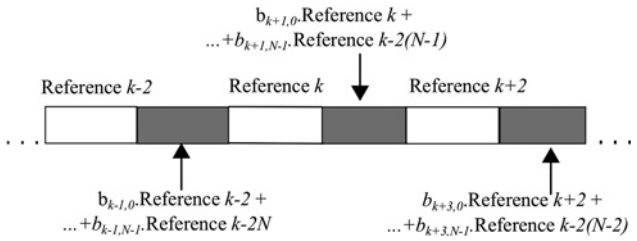

Fig. 2 *Transmitted frames in VHE-DCSK*

chaotic sequence generator and N delay components. Its complexity evolves proportionally to the number N of bits to be transmitted. For $N=1$ and $N=2$, the emitter structures obtained correspond to those of the DCSK and HE-DCSK systems, respectively.

In our proposal, data frames consisting of two TSs of similar size with duration $M \times T_e$ are transmitted, where M is the spreading factor and T_e is the sampling period or chip duration (see Fig. 2). During the first TS, a reference sequence is transmitted. The second TS transmits N information bits, which are modulated separately by N chaotic sequences. One of these chaotic sequences is the reference sequence transmitted during the first TS of the current frame; the other $N-1$ chaotic sequences correspond to the reference sequences transmitted during the previous $N-1$ frames. The sum of all these modulated signals is transmitted during the second TS. In the rest of this paper, vectors are in bold, while samples are in normal.

Chaotic samples are: $c_n(n=-\infty, \ldots, +\infty)$

During TS number k(k even), only chaotic reference sequence of length M is transmitted. The chaotic transmitted signal is represented by a vector($1 \times M$)

$$\boldsymbol{C}_k = [c_{kM}, c_{kM+1}, \ldots, c_{kM+(M-1)}], \quad (k \text{ even}) \tag{1}$$

Data bearing samples are $e_n(n=-\infty, \ldots, +\infty)$. During TS number k (k odd), data are transmitted. The emitted signal is represented by a vector ($1 \times M$):

$$\boldsymbol{E}_k = [e_{kM}, e_{kM+1}, \ldots, e_{kM+(M-1)}], \quad (k \text{ odd}) \tag{2}$$

Data transmitted during this kth TS are $b_{k,u}(u=0 \text{ to } N-1)$, where N is the number of bits transmitted in the odd TSs

$$\boldsymbol{E}_k = \sum_{u=0}^{N-1} b_{k,u} \boldsymbol{C}_{k-2u-1}. \tag{3}$$

$$e_{kM+i} = \sum_{u=0}^{N-1} b_{k,u} c_{(k-2u-1)M+i}, \quad i=0, 1, \ldots, M-1 \tag{4}$$

The signal transmitted during TS k is represented by a vector ($1 \times M$)

$$\boldsymbol{S}_k = [s_{kM}, s_{kM+1}, \ldots, s_{kM+(M-1)}] = \begin{cases} \boldsymbol{C}_k, & k \text{ even} \\ \boldsymbol{E}_k, & k \text{ odd.} \end{cases}$$

In the following two sections, we give the receiver scheme and the performances analysis in the two cases: AWGN channel and a two-ray Rayleigh fading channel.

3 AWGN channel case

3.1 VHE-DCSK receiver scheme

The receiver adopted in this paper is a non-coherent one. It is based on the correlation between chaotic references and data TSs. Fig. 3 shows the generalised structure of the proposed receiver. Each branch of the receiver demodulates one information bit. In this paper, we suppose that the receiver knows perfectly the beginning of each TS. This kind of synchronisation is easily realised by means of autocorrelation of the incoming signal. The received signal at the output of this channel is

$$r_n = g s_n + \varepsilon_n, \tag{5}$$

where g is a real channel gain and without loss of generality is taken equal to 1.ε_n is zero-mean real stationary Gaussian random process with variance $N_0/2$.

Knowing that the received signal vector is real, we obtain the pth bit of the kth TS (k odd) by multiplying the received signal vector $\boldsymbol{R}_k$ ($1 \times M$) by $\boldsymbol{R}_{k-2p-1}^{\mathrm{T}}(1 \times M)$. The decision variable is

$$Z_{k,p} = \Re\left[\boldsymbol{R}_k \boldsymbol{R}_{k-2p-1}^{\mathrm{H}}\right] = \boldsymbol{R}_k \boldsymbol{R}_{k-2p-1}^{\mathrm{T}}, \quad p=0, 1, \ldots, N-1 \tag{6}$$

where H, T and $\Re(.)$ are the conjugate transpose, transpose and the real operators, respectively. (see (7))

where (see (8))

The first term in (7) corresponds to the useful signal, from which the information can be easily deduced. It may be positive or negative, depending on whether the transmitted symbol is +1 or −1. The remaining terms consist of noise and multiuser interferences. There are exactly $(N-1)$ components of multiuser interferences from the correlation between two different chaotic sequences, $(N+1)$ noise components from the correlation between the noise and chaotic sequences as well as one term related to the noise correlation. The useful signal corresponds to the reference chaotic signal energy computed on one TS. Due to the used chaotic sequence properties, this energy can change from one bit to another; this is another

$$\begin{aligned} Z_{k,p} = \boldsymbol{R}_k \boldsymbol{R}_{k-2p-1}^{\mathrm{T}}, \quad p=0, 1, \ldots, N-1 &= \sum_{i=0}^{M-1} \left(e_{kM+i} + \varepsilon_{kM+i}\right) \times \left(c_{(k-2p-1)M+i} + \varepsilon_{(k-2p-1)M+i}\right) \\ &= \sum_{i=0}^{M-1} \left(\sum_{u=0}^{N-1} b_{k,u} c_{(k-2u-1)M+i} + \varepsilon_{kM+i} \right) \times \left(c_{(k-2p-1)M+i} + \varepsilon_{(k-2p-1)M+i}\right) = b_{k,p} \sum_{i=0}^{M-1} c_{(k-2p-1)M+i}^2 + \gamma_{k,p}. \end{aligned} \tag{7}$$

$$\gamma_{k,p} = \sum_{i=0}^{M-1} \sum_{\substack{u=0 \\ u \neq p}}^{N-1} b_{k,u} c_{(k-2u-1)M+i} c_{(k-2p-1)M+i} + \sum_{i=0}^{M-1} \sum_{u=0}^{N-1} b_{k,u} c_{(k-2u-1)M+i} \varepsilon_{(k-2p-1)M+i} + \sum_{i=0}^{M-1} \varepsilon_{kM+i} c_{(k-2p-1)M+i} + \sum_{i=0}^{M-1} \varepsilon_{kM+i} \varepsilon_{(k-2p-1)M+i}. \tag{8}$$

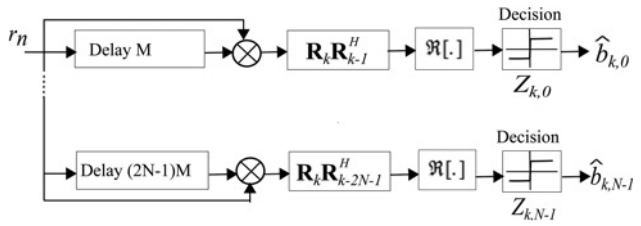

Fig. 3 *Receiver structure*

source of disturbance for the received signal. Finally, each bit can be decoded using the following equation

$$\hat{b}_{k,p} = \text{Sign}(Z_{k,p}). \tag{9}$$

3.2 Emitter/receiver implementation

Figs. 1 and 3 show the functional schemes of the emitter/receiver using analogue delay line components, which are complicated hardware components to implement. In order to use less complex hardware components, the emitter/receiver implementation should be done using a digital implementation. At the emitter side, the digital implementation requires:

- At each TS: generation of M chaotic samples using (10).
- Storage of these M chaotic samples in memory ($N \times M$ chaotic samples have to be stored).
- Generation of signal s_n using (3) and (4), where past chaotic samples will be read in the corresponding memory.
- Digital-to-analogue conversion of signal s_n.

On the receiver side, the received signal at the output of the channel passes through an analogue-to-digital converter and a digital implementation will be also adopted. Here also, a memory with length $2 \times M \times N$ is necessary in order to perform computation of the decision variable of (6).

3.3 Performance analysis in AWGN

The Gaussian approach [15–17] is used in this section to evaluate the theoretical performance of the proposed VHE-DCSK system in terms of the BER. It is well known that this approach gives good results for sufficiently large spreading factors, which are desirable in a typical scenario of spread spectrum communication. For smaller spreading factors, other approaches such as [16, 18] can be used, which are not discussed here. Throughout this paper, the second-order Chebyshev polynomial function (CPF) is chosen due to its simplicity as chaotic sequences generator. This map is defined as follows

$$c_{k+1} = 1 - 2c_k^2. \tag{10}$$

where $-1 \leqslant c_k \leqslant +1$.

Chaotic sequences generated from this map are normalised in order to be zero mean with unitary variance, i.e.

$$E[c_k] = 0, \quad \text{Var}[c_k] = E[c_k^2] = 1,$$

where $E[.]$ and Var[.] are the expectation and the variance operator, respectively. Higher orders moments are derived in [18] and are equal to: $\text{Var}[c_k^2] = 0.5$.

In (7), the noise plus interference terms $\gamma_{k,p}$ can be considered as Gaussian if central limit theorem can be applied. Due to the correlation between c_i and c_{i+k} decreases rapidly and ε_i is independent from $\varepsilon_j(\forall i, \forall j)$, for sufficiently high values of M, this assumption is verified. Equation (7) can be written as follows

$$Z_{k,p} = b_{k,p}A + b_{k,p}\Psi + \gamma_{k,p}, \tag{11}$$

where

$$\Psi = \sum_{i=0}^{M-1} c_{(k-2p-1)M+i}^2 - A,$$

and

$$A = E\left[\sum_{i=0}^{M-1} c_{(k-2p-1)M+i}^2\right]. \tag{12}$$

The proposed system allows transmitting N bits during two TSs. The average energy per bit E_b is then

$$E_b = \frac{M(N+1)}{N}E[c^2] = \frac{M(N+1)}{N}. \tag{13}$$

According to (12) and (13), it is easy to obtain

$$A = ME[c_{(k-2p-1)M+i}^2] = \frac{NE_b}{(N+1)}.$$

With all the previous assumptions and based on the analytical results obtained in [13, 15], the cross correlations between all the sum terms of (7) are equal to zero. The decision variable $Z_{k,p}$ may easily be characterised by its variance $\text{Var}[Z_{k,p}]$, which can be estimated by calculating the variance of $b_{k,p}\Psi + \gamma_{k,p}$, such that

$$\text{Var}[Z_{k,p}] = \text{Var}[b_{k,p}\Psi + \gamma_{k,p}] = \text{Var}[\Psi] + \text{Var}[\gamma_{k,p}], \tag{14}$$

where

$$\text{Var}[\Psi] = M\text{Var}[c_{(k-2p-1)M+i}^2] = \frac{N^2E_b^2}{2M(N+1)^2}. \tag{15}$$

Knowing that the noise has a variance equal to $N_0/2$, we obtain

$$\text{Var}[\gamma_{k,p}] = \frac{E_b^2N^2(N-1)}{M(N+1)^2} + \frac{NE_bN_0}{2} + \frac{MN_0^2}{4}. \tag{16}$$

The BERs performance calculated for all the decoded bits are similar, consequently, the BER performance of VHE-DCSK system is as follows: (see (17))

where erfc (.) is the complementary error function [19].

If we replace N with 2 and 1, respectively, we obtain the respective expressions of the bit error rates of both systems HE-DCSK [13] and DCSK [3] of the literature when CPF map is used.

4 Two-ray Rayleigh fading channel case

4.1 System model

In this subsection, we evaluate our system over a commonly used channel model, named as the two-ray Rayleigh fading channel model [20, 21]. Fig. 4 shows the scheme of this channel model.

$$\text{BER}_{\text{AWGN}} = P(\Psi + \gamma_{k,p} > A) = 0.5\text{erfc}\left(\sqrt{\left(\frac{E_b}{N^2N_0}\right)\left(\frac{E_b(2N-1)}{N^2N_0M} + \frac{(1+N)^2}{N^3} + \frac{MN_0(N+1)^2}{2N^4E_b}\right)^{-1}}\right). \tag{17}$$

The output of this channel is

$$\text{output} = g_1 s_n + g_2 s_{n-\tau}. \tag{18}$$

where τ is an integer. Without loss of generality, we consider that the time delay of Fig. 4 is equal to

$$\text{Time delay} = \tau \times T_e(\tau \text{ integer}).$$

g_1 and g_2 are two complex channel gains with Rayleigh module and a uniformly distributed phase on $[0, 2\pi]$.

The received signal is

$$r_n = g_1 s_n + g_2 s_{n-\tau} + \varepsilon_n, \tag{19}$$

where ε_n is a complex circular white Gaussian noise with variance $N_0/2$ for its real and imaginary parts.

At the receiver side, a correlation detection is adopted to extract each information as shown in Fig. 3. We obtain the pth bit of the kth TS (k odd) by multiplying the received signal vector $\boldsymbol{R}_k$ $(1 \times M)$ by the conjugate transpose of its delayed version $\boldsymbol{R}_{k-2p-1}$ $(1 \times M)$.

4.2 Performance analysis

The correlator output $Z_{k,p}$ is presented as the real part of (see (20))

In the following, we consider that the time delay τ between the two rays is very small compared with the symbol duration $0 < \tau \ll 2M$. Therefore, in (20), comparing its first and second parts, the former can be neglected. Using the same approximation used in [21], (20) can be approximated as (see (21))

where (see (22))

Looking at the decision variable given in (21) and (22), we see that only the first two terms comprise of the useful signal, while all other ones are interferences that arise from different cross products of different reference sequences and different Gaussian noises sequences.

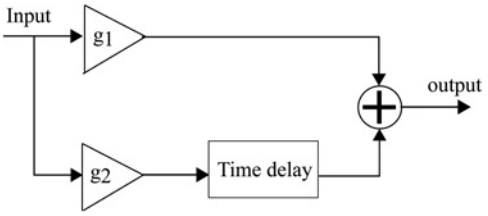

Fig. 4 *Two-ray Rayleigh fading channel model*

As in AWGN channel case, each bit can be decoded using (9).

As we have said previously, all correlators outputs can be considered as Gaussian distributed and they can be fully characterised by their variances and mean values. In order to simplify the analysis, (21) can be transformed as

$$Z_{k,p} = b_{k,p} A + b_{k,p} \Psi + \gamma_{k,p}, \tag{23}$$

where

$$\Psi = \sum_{i=0}^{M-1} \left(|g_1|^2 c^2_{(k-2p-1)M+i} + |g_2|^2 c^2_{(k-2p-1)M-\tau+i} \right) - A,$$

and

$$\begin{aligned} A &= \mathrm{E}\left[\sum_{i=0}^{M-1} \left(|g_1|^2 c^2_{(k-2p-1)M+i} + |g_2|^2 c^2_{(k-2p-1)M-\tau+i} \right) \right] \\ &= M(|g_1|^2 + |g_2|^2) E[c_k^2] = \frac{N E_b (|g_1|^2 + |g_2|^2)}{(N+1)}. \end{aligned} \tag{24}$$

Variance of $Z_{k,p}$ can be estimated by evaluating the variance of $b_{k,p}\Psi + \gamma_{k,p}$ as in (14), where

$$\begin{aligned} Z_{k,p} = \Re\left[\boldsymbol{R}_k \boldsymbol{R}^{\mathrm{H}}_{k-2p-1} \right], \quad p = 0, 1, \ldots, N-1 = \Re\Bigg[& \sum_{i=0}^{\tau-1} \left(\sum_{u=0}^{N-1} g_1 b_{k,u} c_{(k-2u-1)M+i} + g_2 c_{kM-\tau+i} + \varepsilon_{kM+i} \right) \\ & \times \left(g_1^* c_{(k-2p-1)M+i} + \sum_{u=0}^{N-1} g_2^* b_{k-2p-2,u} c_{(k-2p-1)M-\tau+i} + \varepsilon^*_{(k-2p-1)M+i} \right) \Bigg] \\ & + \Re\left[\sum_{i=\tau}^{M-1} \left(\sum_{u=0}^{N-1} g_1 b_{k,u} c_{(k-2u-1)M+i} + \sum_{u=0}^{N-1} g_2 b_{k,u} c_{(k-2u-1)M-\tau+i} + \varepsilon_{kM+i} \right) \times (g_1^* c_{(k-2p-1)M+i} + g_2^* c_{(k-2p-1)M-\tau+i} + \varepsilon^*_{(k-2p-1)M+i}) \right]. \end{aligned} \tag{20}$$

$$\begin{aligned} Z_{k,p} &\simeq \Re\left[\sum_{i=0}^{M-1} \left(\sum_{u=0}^{N-1} g_1 b_{k,u} c_{(k-2u-1)M+i} + \sum_{u=0}^{N-1} g_2 b_{k,u} c_{(k-2u-1)M-\tau+i} + \varepsilon_{kM+i} \right) \times (g_1^* c_{(k-2p-1)M+i} + g_2^* c_{(k-2p-1)M-\tau+i} + \varepsilon^*_{(k-2p-1)M+i}) \right] \\ &\simeq \Re\left[\sum_{i=0}^{M-1} (g_1 g_1^* b_{k,p} c^2_{(k-2p-1)M+i} + g_2 g_2^* b_{k,p} c^2_{(k-2p-1)M-\tau+i}) \right] + \gamma_{k,p}. \end{aligned} \tag{21}$$

$$\begin{aligned} \gamma_{k,p} = \Re\Bigg[& \sum_{i=0}^{M-1} \sum_{\substack{u=0 \\ u \neq p}}^{N-1} g_1 g_1^* b_{k,u} c_{(k-2u-1)M+i} c_{(k-2p-1)M+i} + \sum_{i=0}^{M-1} \sum_{u=0}^{N-1} g_1 g_2^* b_{k,u} c_{(k-2u-1)M+i} c^*_{(k-2p-1)M-\tau+i} + \sum_{i=0}^{M-1} \sum_{u=0}^{N-1} g_1 b_{k,u} c_{(k-2u-1)M+i} \varepsilon^*_{(k-2p-1)M+i} \\ & + \sum_{i=0}^{M-1} \sum_{u=0}^{N-1} g_2 g_1^* b_{k,u} c_{(k-2u-1)M-\tau+i} c_{(k-2p-1)M+i} + \sum_{i=0}^{M-1} \sum_{\substack{u=0 \\ u \neq p}}^{N-1} g_2 g_2^* b_{k,u} c_{(k-2u-1)M-\tau+i} c_{(k-2p-1)M-\tau+i} \\ & + \sum_{i=0}^{M-1} \sum_{u=0}^{N-1} g_2 b_{k,u} c_{(k-2u-1)M-\tau+i} \varepsilon^*_{(k-2p-1)M+i} + \sum_{i=0}^{M-1} g_1^* c_{(k-2p-1)M+i} \varepsilon_{kM+i} + \sum_{i=0}^{M-1} g_2^* c_{(k-2p-1)M-\tau+i} \varepsilon_{kM+i} + \sum_{i=0}^{M-1} \varepsilon^*_{(k-2p-1)M+i} \varepsilon_{kM+i} \Bigg]. \end{aligned} \tag{22}$$

$$\mathrm{Var}[\Psi] = M(|g_1|^4 + |g_2|^4)\mathrm{Var}[c_k^2] = \frac{N^2 E_b^2(|g_1|^4 + |g_2|^4)}{2M(N+1)^2}. \quad (25)$$

If $g_1 = a + jb$ and $g_2 = c + jd$ and knowing that the noise has a variance of $N_0/2$ for its real and imaginary parts, we easily obtain

$$\mathrm{Var}[\gamma_{k,p}] = \frac{E_b^2 N^2((N-1)(|g_1|^4 + |g_2|^4) + 2N(ac+bd)^2)}{(N+1)^2 M} + \frac{NN_0E_b(|g_1|^2 + |g_2|^2)}{2} + \frac{MN_0^2}{2}. \quad (26)$$

$$\mathrm{BER}_{2\text{-Ray}}(g_1, g_2) = P(\Psi + \gamma_{k,p} > A) = 0.5\mathrm{erfc}\left[\left(\frac{(2N-1)(|g_1|^4+|g_2|^4)+4N(ac+bd)^2}{M(|g_1|^2+|g_2|^2)^2} + \frac{N_0(N+1)^2}{NE_b(|g_1|^2+|g_2|^2)} + \frac{MN_0^2(N+1)^2}{N^2E_b^2(|g_1|^2+|g_2|^2)^2}\right)^{(-1/2)}\right]. \quad (27)$$

Equation (27) gives the instantaneous BER of VHE-DCSK in the case of two-ray Rayleigh fading channel for given gains g_1 and g_2.

The first term in (27) can be written as follows

$$\begin{aligned}&\frac{(2N-1)(|g_1|^4 + |g_2|^4) + 4N(ac+bd)^2}{M(|g_1|^2 + |g_2|^2)^2} \\ &= \frac{(2N-1)(|g_1|^2 + |g_2|^2)^2}{M(|g_1|^2 + |g_2|^2)^2} + \frac{2(a^2+b^2)(c^2+d^2)}{M(|g_1|^2 + |g_2|^2)^2} \\ &\quad - \frac{4N(ad-bc)^2}{M(|g_1|^2 + |g_2|^2)^2} \\ &\simeq \frac{2N-1}{M}. \end{aligned} \quad (28)$$

Since, for large M, the second and the third terms of (28) can be neglected. After simplification, we obtain

$$\begin{aligned}&\mathrm{BER}_{2\text{-Ray}}(g_1, g_2) = 0.5\mathrm{erfc} \\ &\left[\left(\frac{2N-1}{M} + \frac{N_0(N+1)^2}{NE_b(|g_1|^2 + |g_2|^2)} + \frac{MN_0^2(N+1)^2}{N^2E_b^2(|g_1|^2 + |g_2|^2)^2}\right)^{(-1/2)}\right] \\ &= 0.5\mathrm{erfc}\left[\left(\frac{2N-1}{M} + \frac{(N+1)^2}{N\lambda_b} + \frac{M(N+1)^2}{N^2\lambda_b^2}\right)^{(-1/2)}\right] \\ &= \mathrm{BER}(\lambda_b). \end{aligned} \quad (29)$$

where $\lambda_b = \left(\left(E_b(|g_1|^2 + |g_2|^2)\right)/N_0\right) = \lambda_1 + \lambda_2$, $\lambda_1 = ((E_b|g_1|^2)/N_0)$ and $\lambda_2 = ((E_b|g_2|^2)/N_0)$.

λ_b is a Chi-square random variable with two degrees of freedom. According to [21], the probability density function (pdf) of λ_b is

$$f(\lambda_b) = \begin{cases} \frac{\lambda_b}{\overline{\lambda}_1^2} e^{-\lambda_b/\overline{\lambda}_1}, & \mathrm{E}[|g_1|^2] = \mathrm{E}[|g_2|^2] \\ \frac{1}{\overline{\lambda}_1 - \overline{\lambda}_2}\left(e^{-\lambda_b/\overline{\lambda}_1} - e^{-\lambda_b/\overline{\lambda}_2}\right), & \mathrm{E}[|g_1|^2] \neq \mathrm{E}[|g_2|^2]. \end{cases} \quad (30)$$

The mean BER is equal to the average of (29) computed for all possible values of λ_b

$$\overline{\mathrm{BER}}_{2\text{-Ray}} = \int_0^\infty \mathrm{BER}(\lambda_b) f(\lambda_b) d_{\lambda_b}. \quad (31)$$

5 Simulation results

In a first part, we will analyse the performances of our system under an AWGN channel. Table 1 summarises the parameters of these simulations, where SNR denotes the signal-to-noise ratio. IC denotes the initial condition of the chaotic map. Nb. paths, Nb. TSs and Nb. bits represent, respectively, the number of paths in the channel, the number of TSs and the number of bits generated during all the simulation time. Finally, Fig. Nb. represents the name of the figure, where the results corresponding to the parameters are plotted.

In the second part, we will analyse the performances of our system when using a two-ray Rayleigh fading channel. Table 2 summarises the parameters of these simulations.

First of all, we will compare the analytical expression of the BER in AWGN channel with simulation results. For this purpose, the values of N and M were set to $N = 4$ and $M = 100$. From the curves obtained (Fig. 5), we note that there is a perfect match between the analytical expression and simulation results in an AWGN channel. This positively helps us to confirm the validity of (17) with a large enough spreading factor M.

Our goal now is to check the performance of the VHE-DCSK system for different values of the spreading factor M and three different values of the number of transmitted bits per TS N. This simulation is done in an AWGN channel with a fixed $(E_b/N_0) = 15$ dB. Simulated and analytical BER performances against spreading factor for different values of N are curved in Fig. 6. Looking at this figure, for small spreading factors, a gap appears between the two curves (simulation and theory); this proves that the Gaussian approach is not precise enough to calculate the performance of spread spectrum systems in the case where small spreading factors are used. Nevertheless, small spreading factors have limited interest in spread spectrum communications. A close observation of the BER values obtained in Fig. 6 suggests that for very small spreading factor values, the BER tends to worsen. This is due to large variations in the average energy per bit E_b. For intermediate values of the spreading factor (between 10 and 100), the BER performance improves until it reaches a minimum. Beyond $M = 100$, calculated and the simulated BERs are in good agreement. For large M, the performance gradually degrades because the noise energy becomes

Table 1 Simulation scheme and parameters (part I)

Nb. paths	Chaotic map	IC	M	N	Nb. TSs	Nb. bits	SNR	Fig. Nb.
1	Chebyshev	0.01	100	4	150,000	300,000	varying	Fig. 5
1	Chebyshev	0.01	varying	4	150,000	300,000	15	Fig. 6
1	Chebyshev	0.01	varying	6	150,000	450,000	15	Fig. 6
1	Chebyshev	0.01	varying	8	150,000	600,000	15	Fig. 6
1	Chebyshev	0.01	100	1	150,000	75,000	varying	Fig. 7
1	Chebyshev	0.01	100	2	150,000	150,000	varying	Fig. 7
1	Chebyshev	0.01	100	4	150,000	300,000	varying	Fig. 7
1	Chebyshev	0.01	100	8	150,000	600,000	varying	Fig. 7
1	Chebyshev	0.01	100	16	150,000	1,200,000	varying	Fig. 7

IET Commun., 2016, Vol. 10, Iss. 17, pp. 2300–2307

Table 2 Simulation scheme and parameters (part II)

Nb. paths	$E[\|g_1\|^2]$	$E[\|g_2\|^2]$	τ	Chaotic map	IC	M	N	Nb. TSs	Nb. bits	SNR	Fig. Nb.
2	1/2	1/2	2	Chebyshev	0.01	100	4	150,000	300,000	varying	Fig. 8
2	10/11	1/11	2	Chebyshev	0.01	100	4	150,000	300,000	varying	Fig. 8
1	1	0	2	Chebyshev	0.01	100	4	150,000	300,000	varying	Fig. 8
2	1/2	1/2	2	Chebyshev	0.01	100	1	150,000	75,000	varying	Fig. 9
2	1/2	1/2	2	Chebyshev	0.01	100	2	150,000	150,000	varying	Fig. 9
2	1/2	1/2	2	Chebyshev	0.01	100	4	150,000	300,000	varying	Fig. 9
2	1/2	1/2	2	Chebyshev	0.01	100	8	150,000	600,000	varying	Fig. 9
2	1/2	1/2	2	Chebyshev	0.01	100	16	150,000	1,200,000	varying	Fig. 9

too high. In fact, the last term in (17) increases with M and the degradation in BER is so important that it will dispel any improvement due to the first term of the same equation. This explanation is true, whatever the value of N, the only difference is that, the greater is the value of N, the worser is the BER.

After, we will compare the performance of our new proposal in terms of BER for different spectral efficiencies to the classical systems DCSK and HE-DCSK. Fig. 7 compares the simulated BER against SNR of VHE-DCSK, HE-DCSK and DCSK in an AWGN channel for different values of N (various spectral efficiencies) and for $M = 100$. For values of $N = 1$, 2 and 4 we obtain almost similar BER for the same occupied bandwidth, while we transmit a different number of bits. For example, for $N = 4$ we have a spectral efficiency four times greater than that of the DCSK system ($N = 1$), while the penalty is lower than 1.5 dB for a BER equal to 10^{-3}. It is also noted that for $N = 2$, this system has a slight better BER performance than that of a DCSK system. This result is in good agreement with the results found by Yang and Jiang [13]. However, for $N = 4$ and 8 the system has better performances than those of the DCSK system for E_b/N_0 less than 14 and 12 dB, respectively. The more N increases, the quicker a noise floor due to interferences emerges. These interferences grow proportionally to N. For example, for $N = 16$, a noise floor of about 10^{-2} appears very quickly. Increasing the value of the spreading factor M may help combat interferences and delay the appearance of the noise floor related to the multiuser interferences.

Now, we analyse the results obtained in two-ray Rayleigh fading channel. For this purpose, we consider the three following cases:

- *Case I:* The average power gain of the first path is equal to the average power gain of the second path $E[|g_1|^2] = (1/2)$ and $E[|g_2|^2] = (1/2)$.
- *Case II:* The average power gain of the first path is 10 dB above the average power gain of the second path $E[|g_1|^2] = (10/11)$ and $E[|g_2|^2] = (1/11)$.
- *Case III:* $E[|g_1|^2] = 1$ and $E[|g_2|^2] = 0$.

For all cases, recall that τ is taken equal to 2, $M = 100$ and $N = 4$. In Fig. 8, we have plotted BER performances against E_b/N_0 for the three cases using Monte Carlo simulations and analytical expression of (31). For the analytical results, a numeric integration has been done using an histogram estimation of the pdf of variable λ_b. First of all, we can see that analytical expressions are closely matching with simulation results. Close matches between simulations and theoretical expressions of (29)–(31) will be valid for small values of τ. When τ is very small compared with $2M$ (meaning that the timing delay is very small compared with the symbol duration), the first term of (20) representing intersymbol interference can be neglected and (21) can be used.

The slope of the BER varies with the three considered cases. For case III, we have a slope of one ($BER \simeq 1/SNR^1$), which is the

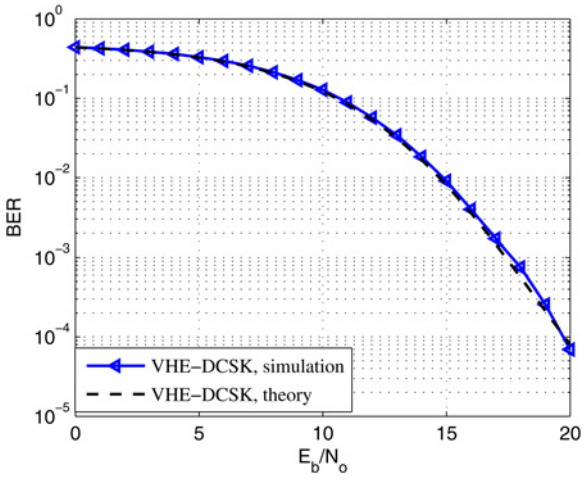

Fig. 5 *Relationship between theoretical BER performances and E_b/N_0 for VHE-DCSK system ($N = 4$) with spreading factor $M = 100$*

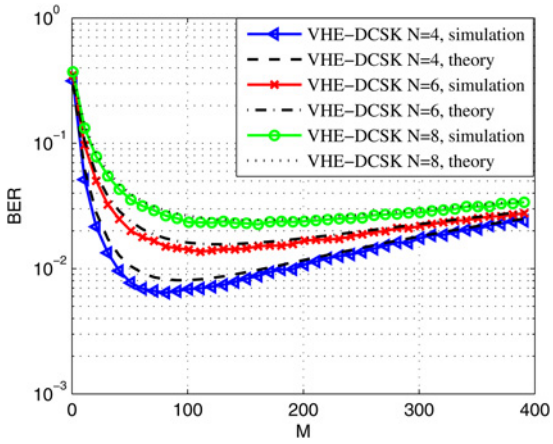

Fig. 6 *BER performances of VHE-DCSK for different values of M and N*

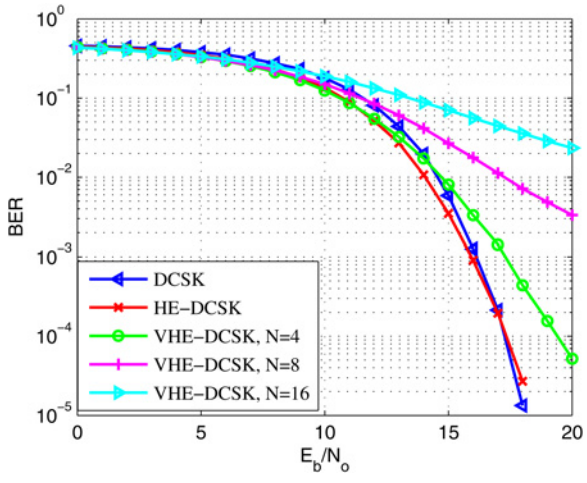

Fig. 7 *BER performances of VHE-DCSK system for various values of N and for various spectral efficiencies over an AWGN channel ($M = 100$)*

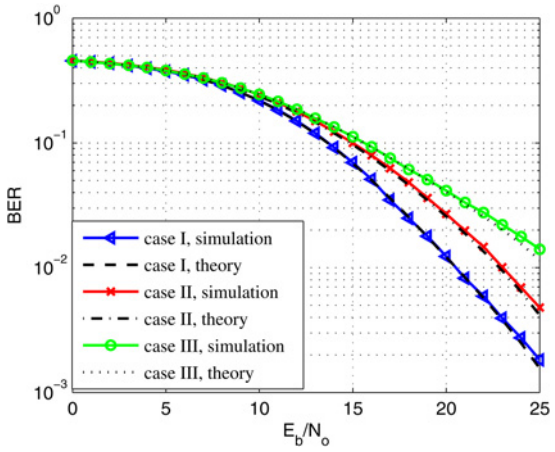

Fig. 8 *BER performances of VHE-DCSK system ($N = 4$) over a two-ray Rayleigh fading channel ($M = 100$, $\tau = 2$)*

classical decrease of BER in a Rayleigh channel, the probability of error decreases by an order of 10^{-1} for an increase of 10 dB in E_b/N_0 (at 25 dB, we have a BER of 2×10^{-2} and at 15 dB, we have a BER of approximately 2×10^{-1}) and, in that case, the diversity order is equal to one. For case I, the receiver receives two versions of the same signal with the same average power gain. Consequently, each path contributes significantly to the decision. In that case, we have a diversity of order 2 (BER $\simeq 1/\text{SNR}^2$). This can be seen in Fig. 8, where the probability of error decreases by an order of roughly 10^{-2} for an increase of 10 dB in E_b/N_0 (at 25 dB, we have a BER of 2×10^{-3} and at 15 dB, we have a BER of 7×10^{-2}). For case II, where there is a dominant path, the BER performance is intermediate between cases I and III. From the results obtained, we can say that increasing diversity allows to combat the effect of multipath Rayleigh fading channel as shown in [22, 23] for DCSK system.

In Fig. 9, we have plotted the BER performances of the VHE-DCSK system over a two-ray Rayleigh fading channel for different spectral efficiencies. The simulated BER performances against SNR for $N = 1$ (DCSK), $N = 2$ (HE-DCSK), $N = 4$, 8, 16 (our proposal) are presented. A two-ray Rayleigh fading channel with two taps as shown in Fig. 4 of this paper, with the same mean power (case I) and a timing delay of $2 \times T_c$ between the two paths has been used. With the AWGN channel (Fig. 7) there was a larger performance penalty when N was increasing: for a BER of 10^{-2} the VHE-DCSK with $N = 8$ was more than 4 dB worse than DCSK. Here, with a multipath Rayleigh channel, if we observe

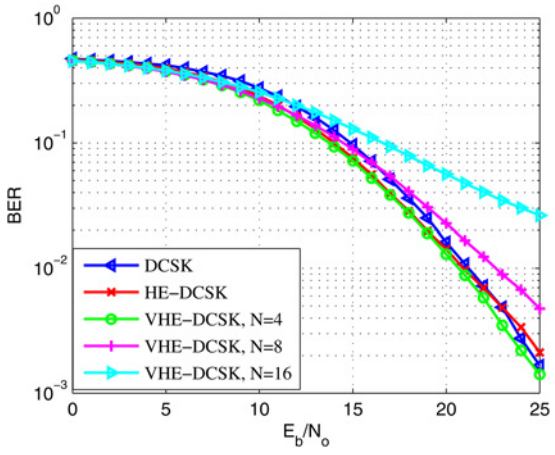

Fig. 9 *BER performances of VHE-DCSK system for various values of N over a two-ray Rayleigh fading channel with similar average power gains($M = 100$, $\tau = 2$)*

carefully all the curves (Fig. 9) obtained for $N = 1$, 2, 4, 8, we notice that they are very similar (a maximum gap of 2 dB exists between the curves for a BER of 10^{-2}). This can be explained by the fact that a Rayleigh channel tends to minor the BER differences experienced in an AWGN channel. Furthermore, it can be observed in Fig. 9 that the slope of the BER curves follows the $1/\text{SNR}^2$ slope because we are in a case where diversity order is equal to 2.

6 Conclusion

In this paper, a new non-coherent communication system, VHE-DCSK, has been presented and analysed. This system is a generalisation of existing HE-DCSK and DCSK systems. VHE-DCSK allows transmitting N bits of data in a two-TS frame using chaotic signals. This new system can significantly increase the spectral efficiency of HE-DCSK and DCSK systems with limited impact on the BER at low and medium SNR. It also offers better security since a chaotic signal is never transmitted twice. Analytical expressions of the BER have been proposed using the Gaussian approximation method in AWGN and two-ray Rayleigh fading channels, which turned out to be in very good agreement with simulation results for medium and large spreading factors. Furthermore, simulations in AWGN channel showed that for moderate E_b/N_0, the VHE-DCSK system exhibits similar BER performance and better spectral efficiency than DCSK one. When the number of bits transmitted per frame, N, and thus spectral efficiency increases, the penalty in terms of E_b/N_0 is limited for BER of the order of 10^{-3}. Nevertheless, interferences between users increase proportionally to N, and hence generate a noise floor for very high values of E_b/N_0. Simulations in the two-ray Rayleigh fading channel showed that increasing the diversity order improved the BER performances and fights against the effect of this kind of channel. Also, for different spectral efficiencies, this kind of channel tends to minor the BER differences obtained in an AWGN channel.

Concerning complexity, the VHE-DCSK system needs additional memory compared with classical DCSK system. Indeed, it is necessary to store the N previous chaotic sequences in order to be able to decode the N data bits of the kth data frame. Compared with the DCSK system, implementation complexity of the VHE-DCSK system is moderate compared with the enhancement of the spectral efficiency.

7 References

1 Parlitz, U., Chua, L.O., Kocarev, L., *et al.*: 'Transmission of digital signals by chaotic synchronization', *Int. J. Bifurcation Chaos*, 1992, **2**, (4), pp. 973–977
2 Dedieu, H., Kennedy, M.P., Hasler, M.: 'Chaos shift keying: modulation and demodulation of a chaotic carrier using self-synchronizing Chua's circuits', *IEEE Trans. Circuits Syst. II*, 1993, **40**, (10), pp. 634–642
3 Kolumbán, G., Vizvári, B., Schwarz, W.: 'Differential chaos shift keying: A robust coding for chaos communication'. NDES'96, Seville, Spain, June 1996, pp. 92–97
4 Lau, F.C.M., Cheong, K.Y., Tse, C.K.: 'Permutation-based DCSK and multiple-access DCSK systems', *IEEE Trans. Circuits Syst. I, Fundam. Theory Appl.*, 2003, **50**, (6), pp. 733–742
5 Galia, Z., Maggio, G.M.: 'Quadrature chaos-shift keying: theory and performance analysis', *IEEE Trans. Circuits Syst. I, Fundam. Theory Appl. (1993–2003)*, 2001, **48**, (12), pp. 1510–1519
6 Kaddoum, G., Soujeri, E., Arcila, C., *et al.*: 'I-DCSK: an improved noncoherent communication system architecture', *IEEE Trans. Circuits Syst. II, Exp. Briefs*, 2015, **62**, (9), pp. 901–905
7 Cai, G., Wang, L., Huang, T.: 'Channel capacity of M-ary differential chaos shift keying modulation over AWGN channel'. ISCIT, Samui Island, Thailand, September 2013, pp. 91–95
8 Chen, P., Wang, L., Chen, G.: 'DDCSK-Walsh coding: a reliable chaotic modulation-based transmission technique', *IEEE Trans. Circuits Syst. II, Exp. Briefs*, 2012, **59**, (2), pp. 128–132
9 Kaddoum, G., Gagnon, F., Richardson, F.D.: 'Design of a secure multi-carrier DCSK system'. ISWCS, Paris, France, August 2012, pp. 964–968
10 Kaddoum, G., Richardson, F.D., Gagnon, F.: 'Design and analysis of a multi-carrier differential chaos shift keying communication system', *IEEE Trans. Commun.*, 2013, **61**, (8), pp. 3281–3291
11 Xu, W.K., Wang, L.: 'A novel differential chaos shift keying modulation scheme', *Int. J. Bifurcation Chaos*, 2011, **21**, (3), pp. 799–814

12 Kaddoum, G., Gagnon, F.: 'Design of a high-data-rate differential chaos shift keying system', *IEEE Trans. Circuits Syst. II, Exp. Briefs*, 2012, **59**, (7), pp. 448–452
13 Yang, H., Jiang, G.P.: 'High-effeciency differential-chaos-shift-keying scheme for chaos-based noncoherent communication', *IEEE Trans. Circuits Syst. II, Exp. Briefs*, 2012, **59**, (5), pp. 312–316
14 Kaddoum, G.: 'Wireless chaos-based communication systems: a comprehensive survey', *IEEE Access*, 2016, **4**, pp. 2621–2648
15 Sushchik, M., Tsimring, L.S., Volkovskii, A.R.: 'Performance analysis of correlation-based communication schemes utilizing chaos', *IEEE Trans. Circuits Syst. I, Fundam. Theory Appl.*, 2000, **47**, (12), pp. 1684–1691
16 Kaddoum, G., Gagnon, F., Chargé, P., *et al*.: 'A generalized BER prediction method for differential chaos shift keying system through different communication channels', *Wireless Pers. Commun.*, 2012, **64**, (2), pp. 425–437
17 Tam, W.M., Lau, F.C.M., Tse, C.K.: 'Generalized correlation-delay-shift-keying scheme for noncoherent chaos-based communication systems', *IEEE Trans. Circuits Syst. I*, 2006, **53**, (3), pp. 712–721
18 Kaddoum, G., Chargé, P., Roviras, D., *et al*.: 'Performance analysis of differential chaos shift keying over an AWGN channel'. ACTEA, Zouk Mosbeh, Lebanon, July 2009, pp. 255–258
19 Sklar, B.: 'Digital communications: Fundamentals and applications' (Prentice-Hall, Englewood Cliffs, NJ, 1988, 1st edn.)
20 Rappaport, T.S.: 'Wireless communications: principles and practice' (Prentice-Hall, Englewood Cliffs, NJ, 1996, 1st edn.)
21 Xia, Y., Tse, C.K., Lau, F.C.M.: 'Performance of differential chaos-shift-keying digital communication systems over multipath fading channel with delay spread', *IEEE Trans. Circuits Syst. II*, 2004, **51**, (12), pp. 680–684
22 Kaddoum, G., Vu, M., Gagnon, F.: 'Performance analysis of differential chaotic shift keying communications in MIMO systems'. ISCAS, Rio de Janeiro, Brazil, May 2011, pp. 1580–1583
23 You, N., Yi, B., Wang, S.: 'Theoretical noise performance of SIMO-DCSK communication schemes'. ISWTA, Kuching, Malaysia, September 2013, pp. 134–137